Recomputation of the Green's functions for tidal loading estimations.

O. Francis
Observatoire Royal de Belgique
3, Avenue Circulaire
B-1180 Bruxelles
Belgique

V. Dehant
Chargée de Recherche au Fonds National de la Recherche Scientifique
Université Catholique de Louvain
2, Chemin du Cyclotron
B 1348 Louvain-la-Neuve
Belgique

Abstract:

The computation of the ocean loading indirect effects is made at each station by using a convolution between the Green's functions and a set of point mass-loads. These Green's functions are computed using a series expansion which presents convergence difficulties. In the present paper the mathematical artifices used by Farrell in 1972 are analysed and tested. A strategy is then proposed and new Green's functions are computed. New theoretical models inside the Earth, thus new Love numbers, are introduced to compute new numerical tables.

Plan

Introduction

The tidal gravimetric observations are collected at the International Center for Earth Tides (ICET). After correction of the local atmospheric pressure effects, when available, the time series are transformed into the frequency domain where they are corrected for the transfer function of the gravimeter itself. The ocean loading effects are then removed. The corrected tidal gravimetric factor δ_c is so determined for about 270 stations. Using the same definition as that of the ICET, latitude dependent theoretical tidal gravimetric factors δ_m can be obtained and compared with the observed ones (Dehant & Ducarme, 1987). There is still a systematic difference of about 0.7% (Figures 1 and 2). In order to understand and interpret the residuals in terms of physics of the Earth interior, the precision of the ocean loading corrections must be increased. These corrections include the direct gravitational attraction of the fluid masses, the deformation of the Earth surface due to their weight and the induced mass redistribution inside the Earth. The modelling of these effects all together requires the knowledge of the ocean tides everywhere on the Earth i.e. corange and cotidal maps which give amplitudes and phases of the ocean tide at every points of a grid. Farrell (1972) developed a method which allows to compute the ocean loading effects at each station. These are usually called the "indirect effects". The procedure is divided into two steps.

The first one consists in computerizing the response of the Earth to a point mass-load considering a particular model for the internal structure of the Earth (see part 1). The different components of the Earth response are tabulated in function of the angular distance between the application point of the load and the observation point. They are called the Green's functions.

For the second step, one considers that an ocean is divided into a set of cells to which a given tidal amplitude and phase are assigned. The mass of each cell is then concentrated at the associated center of figure and a convolution using these masses and the Green's functions is performed in order to compute the total response of the Earth (see part II).

It must also be mentioned that the ocean and atmospheric loading effects are not only perturbing gravity data but they are also important for precise geophysical and geodetical data.

In part I of this paper, we present a critical analysis of the Farrell's method for the computation of the Green's functions and new numerical values are obtained for different rheological models inside the Earth. The new results are used in part II to computerize indirect effects at different stations.

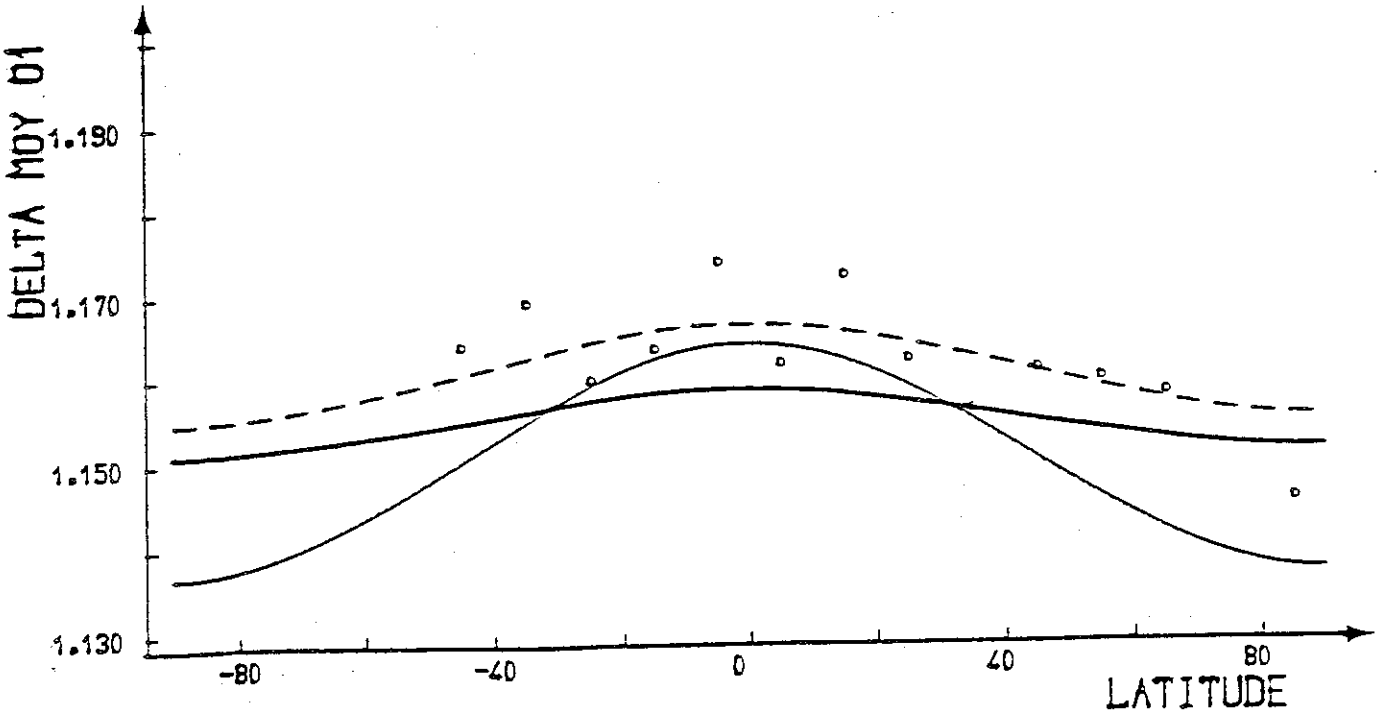

Figure 1: Results for O_1 using the 1066A model like in (5). Points = means computed for each span of 10 degrees from the observed tidal gravimetric factors (ICET data bank). Dashed line = curve deduced from the observed δ by regression; fine curve = δ from Wahr's definition; thick curve = δ from the present paper definition.

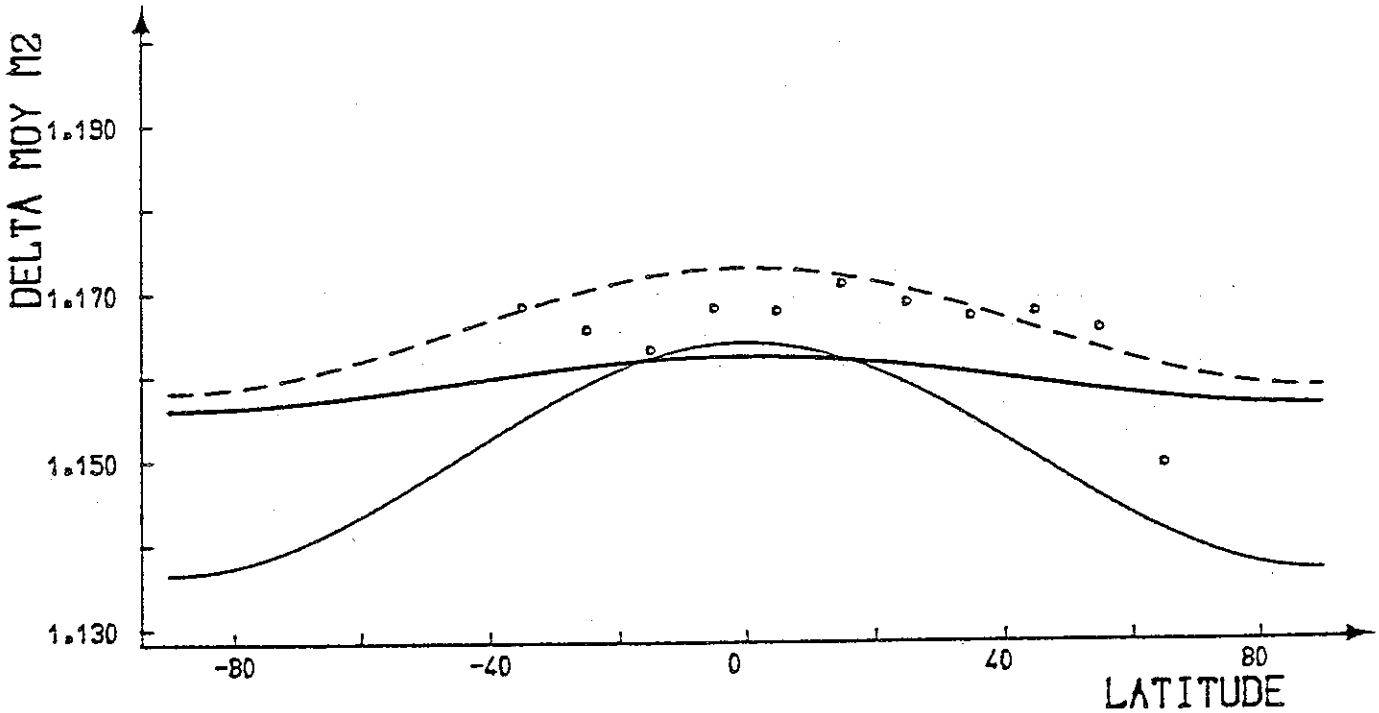

Figure 2: Results for M_2 using the 1066A model like in (5). Same comments as in figure 1.

1. Definition of Love numbers and Green's functions

The Love and Shida numbers have been introduced in the case of a spherical non rotating Earth. They are dimensionless numbers which characterize the Earth's response to the luni-solar attraction. One defines them as Earth's transfer functions between these characteristics and the external tidal potential or its derivative.

They have been generalized in the case of an external mass-load potential. In this case, they are called mass-load Love numbers and are usually distinguished by a superscript prime.

The Earth response to a mass-load is computed by integrating the equation of motion, the stress-strain relationship and Poisson's equation inside the Earth, from the center to the surface. These equations are parameterized by the rheological properties of the Earth and thus load Love numbers depend on the "seismological model".

Because the mass-load potential can be developed in Legendre's polynomials, a same expansion can be applied to transform the vectorial equations (Partial Differential Equations) into scalar equations (Ordinary Differential Equations of the first order in d/dr). Mass-load Love numbers are obtained in this way for each fixed degree of the potential.

The load Love numbers are used in the computation of the Green's functions. These functions represent the response of the Earth at an observation point to an external mass-load point at an angular distance θ.

The Green's functions form three groups:

(a) the horizontal and vertical displacements,
(b) the horizontal and vertical accelerations,
(c) the strain tensor components.

Some of the mathematical expressions can be found in Farrell's paper (1972). The others can be found in Melchior (1983). We reproduce them in table 1.

TABLE 1: Mathematical expression of the Green's functions

radial displacement :

$$u(\theta) = \frac{a}{m_e} \sum_{n=0}^{\infty} h'_n P_n(\cos\theta) \tag{1}$$

horizontal displacement :

$$v(\theta) = \frac{a}{m_e} \sum_{n=0}^{\infty} l'_n \frac{\partial P_n(\cos\theta)}{\partial\theta} \tag{2}$$

gravity acceleration :

$$g(\theta) = \frac{g}{m_e} \sum_{n=0}^{\infty} (n + 2h'_n - n(n+1)k'_n) P_n(\cos\theta) \tag{3}$$

tilt :

$$t(\theta) = -\frac{1}{m_e} \sum_{n=0}^{\infty} (1 + k'_n - h'_n) \frac{\partial P_n(\cos\theta)}{\partial\theta} \tag{4}$$

astronomical tilt :

$$A(\theta) = -\frac{1}{m_e} \sum_{n=0}^{\infty} (1 + k'_n - l'_n) \frac{\partial P_n(\cos\theta)}{\partial\theta} \tag{5}$$

strain :

$$\epsilon_{\theta\theta} = \frac{u}{a} + \frac{1}{m_e} \sum_{n=0}^{\infty} l'_n \frac{\partial^2 P_n(\cos\theta)}{\partial\theta^2} \tag{6}$$

where a is the mean radius of the Earth, m_e is the total mass of the Earth normalised with respect to unit mass , θ is the angular distance, h'_n, k'_n and l'_n are the load Love numbers and P_n are the Legendre's polynomials.

2. Numerical Computations

2.1. Inputs:

In order to compute the Green's functions all the elements of the mathematical expressions presented in Table 1 must be numerically evaluated. These elements are some fundamental constants, the Love numbers and the Legendre polynomials.

a) The constants:

The numerical computation of the Green's functions requires the knowledge of the mean radius of the Earth a, the mean gravity at the surface g and the Earth total mass m_e. Different reasonable values of the constants have been considered. We found relative errors up to $5\ 10^{-4}$ on the Green's functions which correspond to the precision on the constant m_e. For the final computations, we take a = 6371 km and g = 9.82 m sec^{-1} as usually and $5974\ 10^{24}$ kg for m_e.

b) The load Love numbers:

In the numerical evaluation, the Love numbers for all degrees up to a fixed number N are required. But Farrell (1972) gives only a list of a few Love numbers in which he suggests to interpolate the missing values. By using different interpolation methods, polynomials or cubic spline interpolation, applied to the raw Love numbers or to their logarithm, we got different results. Due to the repartition of the Love numbers computed by Farrell, an interpolation on the logarithmic values seems to be safer. This is illustrated in Figure 3. In the logarithm case, the relative difference on the Green's functions obtained by using the 6 points Lagrange interpolation and by the cubic-spline interpolation is of the order of $5\ 10^{-3}$.

c) The Legendre polynomials:

In order to compute the Legendre polynomials, we use a formula relating one degree, n, to the two previous degrees, n-1 and n-2. The stability of this formula could be verified using the true values of the Legendre polynomials at different orders for $\theta = 90^\circ$ and $\theta = 180^\circ$ which are well known. The results are presented in Table 2 and 3 respectively. It can be concluded that the relative error is of the order of $5\ 10^{-10}$ and is thus negligeable.

Table 2: Numerical values of the Legendre polynomials corresponding to $\theta = 90^\circ$.

n	P_n exact	P_n obtained from the recursive formula
101	0	$0.41023 \ldots 10^{-10}$
1001	0	$-0.12886 \ldots 10^{-10}$
5001	0	$-0.28790 \ldots 10^{-9}$
10001	0	$-0.39694 \ldots 10^{-9}$

Table 3: Numerical values of the Legendre polynomials corresponding to $\theta = 180^\circ$

n	P_n exact	P_n obtained from the recursive formula
101	1	1.00000000000000173
1001	1	1.00000000000019887
5001	1	1.00000000000518078
10001	1	1.00000000002076986

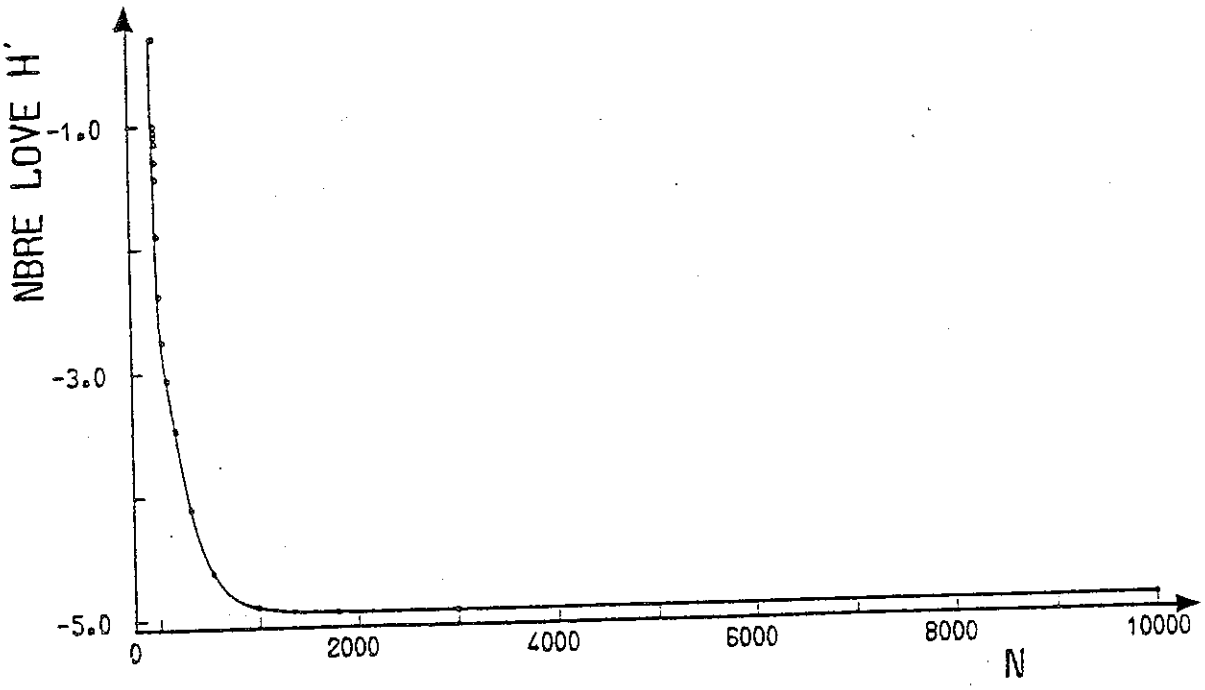

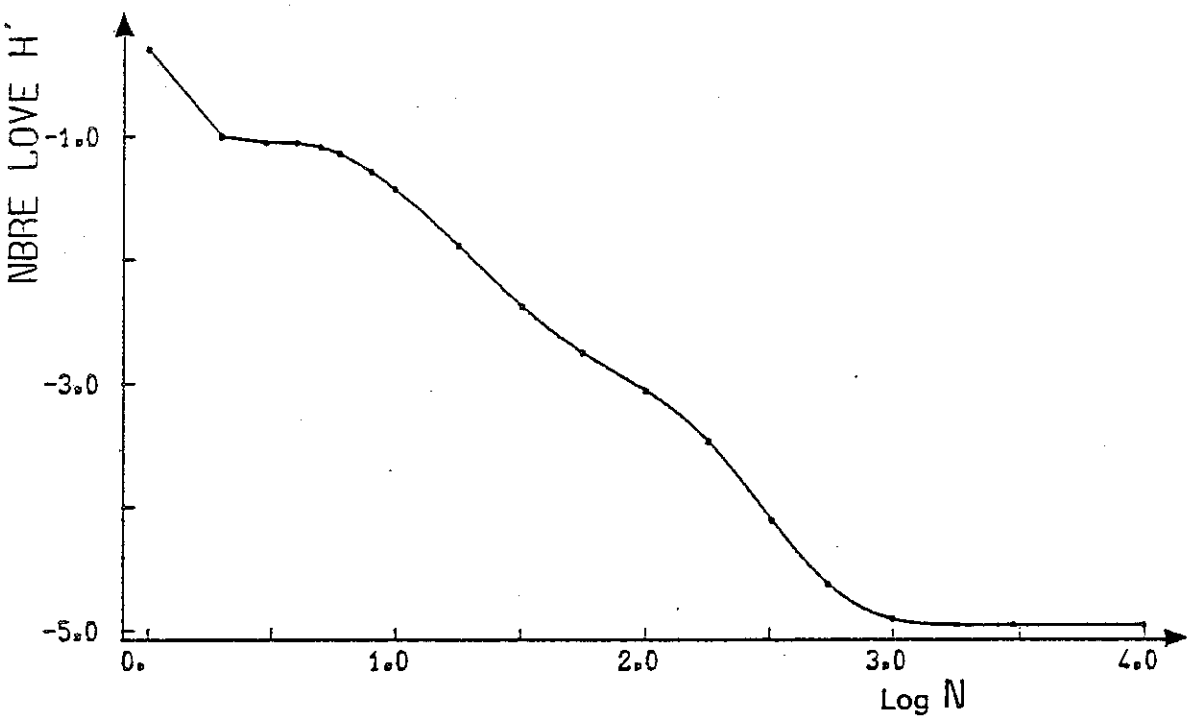

Figure 3: Load Love number h' tabulated by Farrell (1972) versus n and log n.

2.2. Summation method

To obtain the Green's functions, it is necessary to compute infinite series of Legendre polynomials weighted by the mass-load Love numbers. All these inputs are described in the previous paragraph.

There are difficulties in the numerical evaluation of the sum due to the slow convergence of the series. These difficulties are related to:
(1) the computer round off errors,
(2) the convergence errors due to truncation in the infinite series,
(3) the amplification in the summation of the errors inherent in the inputs.

Among all the inputs the errors on the Love numbers have the most important part in this amplification (3). These load Love numbers are provided with an absolute error of the order of $5\ 10^{-4}$ in Farrell's paper.

One of us (Francis, 1987) computed the maximum absolute errors on the sum. In all the cases except for small θ (see below) these maximum absolute errors are greater than the final results.

The first difficulty (1) can be removed easily by increasing the number of digits in the computation. As far as the next two difficulties are concerned, a compromise must be found because, in order to reduce the convergence errors (2), a maximum of terms in the series should be summed up; on the other hand, the reduction of the third kind of errors (3) requires a minimum of terms. For that purpose, mathematical "artifices" must be used, as Farrell (1972) already mentioned.
The objective of the present section is to review and test these artifices in order to deduce a more appropriate strategy for the computation of the Green's functions.

2.2.1. Kummer's transformation

Based on the well known asymptotic behaviour of the Love numbers (precisely of h'_n, nk'_n and nl'_n), the Green's functions can be rewritten. The radial displacement, for example is expressed by:

$$u_r = \frac{ah'_\infty}{m_e} \sum_{n=0}^{\infty} P_n(\cos\theta) + \frac{a}{m_e} \sum_{n=0}^{\infty} (h'_n - h'_\infty) P_n(\cos\theta) \qquad (8)$$

where a, m_e, θ are defined in Table 1 and h_∞ is the asymptotic value.
The advantage of this procedure is that the first part can be evaluated exactly and the Legendre polynomials in the second part are now weighted by $(h'_n - h'_\infty)$ which is a more rapidly decreasing function of n. Thus, for the same fixed precision, the number of terms in the summation will be smaller.

Table 4 displays the Green's functions computed using the Kummer's transformation alone. It can be seen that the values are not coherent with respect to the Farrell's results which include other mathematical artifices. Moreover, for the tilt, the values are even out of range when $\theta > 5^{\circ}$.

2.2.2. Euler's transformation

The Kummer's transformation is the first step in the compromise we are looking for. The second step is to apply the Euler's transformation. This method is a standard technique to rapidly sum alternating series. Thus the Green's functions must be transformed into alternating series. The most logical way is to construct them by using the cosine-like behaviour of the Legendre polynomials.

Our first idea was to make a test on the sign on the polynomials. But Farrell (1972) uses the following formula:

$$u_r = \sum_{i=0}^{M} a_i(\theta)$$

where $M = N \left\langle \frac{\theta}{\pi} \right\rangle$, the symbol $\langle\rangle$ indicates the nearest integer,

$$a_i(\theta) = \sum_{n=j(i)}^{k(i)} (h'_n - h'_\infty) P_n(\cos\theta)$$

$$\text{with } j(0) = 0,\ j(i) = k(i-1) + 1,$$

$$k(0) = \left\langle \frac{\pi}{4\theta} \right\rangle \text{ and } k(i) = j(i) + \left\langle \frac{\pi}{\theta} \right\rangle$$

In this formula, the number of terms in each partial sum, $a_i(\theta)$, is always the same because one always incrementes by the constant $\langle\pi/\theta\rangle$; however, if one uses a sign test to construct the partial sums , one sees that the number of successive Legendre polynomials of the same sign in each sub-sum $a_i(\theta)$ is not constant. But then, in the Farrell's case and when the number of terms in the partial sum is small (when θ is large, π/θ becomes small), the a_i have no more the same magnitude. In addition, the sign alternation is no more respected.

For small angular distances θ, both methods give the same results (see Table 5). But for angles higher than about 100°, there are some differences at the second or third decimal. The corresponding number of partial sums in the numerical computation becomes very different.

To discreminate between both choices, let us write down the necessary conditions to apply the Euler's transformation:

Table 4: Green's functions computed by using only the Kummer's transformation. The same normalisation as Farrell (1972) is adopted. Only the elastic part of the Green's function are tabulated as Farrell did. This is noticed by the subscript E.

The lines show the decimals from which the absolute differences with respect to Farrell's results are higher than 0.5.

θ, deg.	$u(\theta)$	$v(\theta)$	$g^E(\theta)$	$t^E(\theta)$	$A^E(\theta)$
.0001	-33.991	-11.367	-78.802	34.006	.000
.0010	-33.857	-11.366	-78.481	34.005	.000
.0100	-32.651	-11.289	-75.632	33.764	.005
.0200	-31.801	-11.177	-73.782	33.120	.010
.0300	-31.107	-11.158	-72.347	33.531	.015
.0400	-30.557	-11.133	-70.213	34.263	.019
.0600	-28.482	-10.885	-66.503	32.522	.028
.0800	-26.850	-10.681	-62.643	33.739	.037
.1000	-25.476	-10.355	-59.805	31.802	.045
.1600	-21.772	-9.365	-51.363	29.209	.067
.2000	-20.017	-8.713	-47.298	26.346	.078
.2500	-18.418	-8.032	-43.501	26.062	.091
.3000	-17.164	-7.473	-40.388	23.576	.102
.4000	-15.733	-6.741	-36.647	20.082	.122
.5000	-14.959	-6.343	-34.428	18.135	.143
.6000	-14.437	-6.156	-32.832	16.262	.165
.8000	-13.676	-6.068	-30.558	18.683	.214
1.0000	-13.015	-5.965	-28.751	14.322	.264
1.2000	-12.298	-5.862	-26.978	17.110	.314
1.6000	-10.958	-5.476	-23.945	13.928	.403
2.0000	-9.755	-4.995	-21.358	10.459	.475
2.5000	-8.502	-4.389	-18.703	11.068	.546
3.0000	-7.531	-3.866	-16.620	13.624	.600
4.0000	-6.136	-3.072	-13.606	17.138	.677
5.0000	-5.257	-2.524	-11.622	9.628	.728
6.0000	-4.674	-2.155	-10.219		.769
7.0000	-4.274	-1.914	-9.188		.810
8.0000	-3.998	-1.760	-8.433		.855
9.0000	-3.803	-1.654	-7.863		.904
10.0000	-3.646	-1.580	-7.390		.956
12.0000	-3.393	-1.501	-6.622		1.080
16.0000	-3.000	-1.437	-5.581		1.368
20.0000	-2.624	-1.386	-4.729		1.676
25.0000	-2.109	-1.309	-3.814		2.076
30.0000	-1.533	-1.212	-2.952		2.449
40.0000	-.294	-.930	-1.431		2.918
50.0000	.843	-.591	-.295		2.784
60.0000	1.671	-.321	.361		2.003
70.0000	2.079	-.216	.536		.730
80.0000	2.053	-.305	.325		-.784
90.0000	1.638	-.559	-.137		-2.288
100.0000	.912	-.898	-.732		-3.581
110.0000	-.039	-1.263	-1.378		-4.539
120.0000	-1.132	-1.546	-2.015		-5.101
130.0000	-2.288	-1.717	-2.606		-5.251
140.0000	-3.439	-1.726	-3.035		-4.994
150.0000	-4.518	-1.550	-3.296		-4.348
160.0000	-5.462	-1.186	-3.283		-3.321
170.0000	-6.210	-.654	-4.293		-1.894
180.0000	-6.193	.000	-3.153		.000

Table 5: The gravimetric Green's function computed using Farrell's intervals (g_F) are compared to those obtained using a sign test (g_T).
N_{it} is the number of partial sums needed to get a fixed precision of $5\ 10^{-4}$.

θ, deg.	$g_F^E(\theta)$	N_{it}	$g_T^E(\theta)$	N_{it}
.0001	-78.802		-78.802	
.0010	-78.481		-78.481	
.0100	-75.632		-75.632	
.0200	-73.782		-73.782	
.0300	-72.013	3	-72.347	3
.0400	-70.111	3	-70.213	8
.0600	-66.484	4	-66.503	8
.0800	-62.931	8	-62.843	11
.1000	-59.669	6	-59.668	5
.1600	-51.486	6	-51.486	7
.2000	-47.351	7	-47.351	7
.2500	-43.403	7	-43.403	7
.3000	-40.483	8	-40.483	8
.4000	-36.640	8	-36.640	8
.5000	-34.352	8	-34.352	9
.6000	-32.814	9	-32.814	10
.8000	-30.573	10	-30.573	11
1.0000	-28.706	10	-28.706	11
1.2000	-27.026	11	-27.026	10
1.6000	-23.983	11	-23.983	10
2.0000	-21.373	11	-21.373	10
2.5000	-18.734	11	-18.734	10
3.0000	-16.650	12	-16.650	10
4.0000	-13.606	10	-13.605	10
5.0000	-11.598	11	-11.598	10
6.0000	-10.211	9	-10.211	10
7.0000	-9.205	10	-9.206	11
8.0000	-8.446	10	-8.442	10
9.0000	-7.853	10	-7.853	11
10.0000	-7.375	10	-7.375	11
12.0000	-6.637	9	-6.638	11
16.0000	-5.571	9	-5.577	10
20.0000	-4.739	11	-4.740	11
25.0000	-3.821	10	-3.825	12
30.0000	-2.962	11	-2.962	11
40.0000	-1.437	18	-1.451	67
50.0000	-.290	28	-.293	88
60.0000	.369	25	.369	11
70.0000	.536	40	.532	157
80.0000	.318	24	.342	87
90.0000	-.143	36	-.143	10
100.0000	-.728	37	-.726	101
110.0000	-1.369	32	-1.351	114
120.0000	-2.012	27	-1.964	307
130.0000	-2.615	17	-2.638	147
140.0000	-3.145	14	-3.141	231
150.0000	-3.593	12	-3.595	136
160.0000	-3.966	13	-3.868	62
170.0000	-4.282	11	-4.282	11
180.0000	-4.555	14	-4.555	14

For the alternate series $\sum_{n=0}^{\infty} (-1)^n a_n$

with $a_n > 0$ for all n.

if the a_n decrease to 0 (1)
if the Δa_n $(=a_n - a_{n-1})$ decrease to 0 (2)
if the $\Delta^2 a_n$ $(= \Delta a_n - \Delta a_{n-1})$ decrease to 0 (3)
and if $\frac{a_{n+1}}{a_n} > -\frac{1}{2}$ (4)

Then the Euler's transformation speeds the convergence.

Condition (4) is verified independently of the determination of the intervals which can be based either on the sign test or on Farrell's choice. In both cases, conditions (1), (2) and (3) are not verified because a_n have a cyclic behaviour. But at the desired precision, the number of partial sums is sufficiently small in Farrell's case to stay in the first cycle and so (1) and (2) are satisfied but (3) is not. The reason why it stops so quickly is that the alternation is not respected. In the sign test case, for the same precision, a higher number of terms must be used as previously mentioned. This number is out of range and this is the reason why we prefer the Farrell choice of interval although there are objections against this method because the hypotheses needed for Euler's transformation, especially the alternation of the series, are not satisfied.

However, this problem of choice arises only for angular distances bigger than about 100°.

2.2.3. Disk factor

The third artifice used by Farrell is the introduction of a disk factor in the second part of the Green's function expression (8). The Green's functions corresponding to a disk load of radius α can be expended in the same way as in the case of the point mass-load, by adding a weight in all the terms of the expansion. This weight is equal to 1 when α tends to zero i.e. for a point mass-load. The second part of expression (8) can than be replaced by:

$$\frac{a}{m_e} \sum_{n=0}^{\infty} \lim_{\alpha \to 0} F_n(\alpha) \, (h'_n - h'_\infty) \, P_n(\cos\theta) \qquad (9)$$

$$\text{with } F_n(\alpha) = \frac{-(1+\cos\alpha)}{n(n+1)\sin\alpha} \frac{\partial P_n(\cos\alpha)}{\partial \alpha}$$

If the limit and the sum are exchanged, the second part of the expression of the Green's functions becomes:

$$\lim_{\alpha \to 0} \frac{a}{m_e} \sum_{n=0}^{\infty} F_n(\alpha) \, (h'_n - h'_\infty) \, P_n(\cos\theta) \qquad (10)$$

The introduction of the disk factor $F_n(\alpha)$ speeds up the convergence of the series, by providing a weight decreasing as $n^{-3/2}$ if α is not too small. At this point arises the question: for α tending to zero, how is the limit numerically estimated?

In Farrell's paper (1972) two methods are suggested:

- First, to compute the Green's functions for different disk factor angles α and extrapolate for α tending to zero.
  Using this method, we have not been able to reproduce the exact results published by Farrell. Table 6 displays differences at the third decimal in the Green's functions. In this table, one can also notice that it was not necessary to extrapolate when small values of α are chosen. Farrell did not comment on this peculiarity. Thus it seems that he did not use this method.

- Secondly, he suggests a simplest way to compute the Green's function, without any limit evaluation. In this case, the disk factor is left in the summation with a particular α angle. The choice of this angle is related to the value of the angular distance θ. Farrell suggests a ratio between the two from 10 to 30. Farrell justifies this choice reasoning in a much simplified case, the Boussinesq plane approximation. In this way, we have been able to reproduce the values tabulated by Farrell except for very small angular distances (see section 2.24).
  Some examples are given in Table 7. However, two objections can be formulated:

  1) The justification for the choice of the α angle is not correct in the spherical case. Even more, the behaviour of the radial displacement $u(\theta)$ for example is different in the two cases: when α increases, in the Boussinesq plane approximation $u(\theta)$ increases, whereas it decreases in the spherical Earth case.

  2) The second objection is that the disk factor has only been introduced in the second part of the sum for the computation of the Green's function (8). But it is necessary to introduce it in the first part of the sum to satisfy the Kummer's transformation. However, if the disk factor is introduced in this part, it becomes impossible to find an exact expression.

Table 6: Comparison between the results of the Green's function $u(\theta)$ obtained by extrapolation for α tending to zero and the Farrell's results (1972).
For the signification of the lines, see Table 4.

θ,deg.	u(θ)
.0200	-31.1969
.0300	-30.9823
.0400	-30.1200
.0600	-28.4175
.0800	-26.8886
.1000	-25.4424
.1600	-21.8818
.2000	-20.0037
.2500	-18.3381
.3000	-17.1199
.4000	-15.7730
.5000	-14.9231
.6000	-14.4330
.8000	-13.6889
1.0000	-12.9999
1.2000	-12.3116
1.6000	-10.9772
2.0000	-9.7611
2.5000	-8.5220
3.0000	-7.5443
4.0000	-6.1336
5.0000	-5.2148
6.0000	-4.6171
7.0000	-4.2180
8.0000	-4.0003
9.0000	-3.7999
10.0000	-3.6411
12.0000	-3.3999
16.0000	-3.0004
20.0000	-2.6224
25.0000	-2.1112
30.0000	-1.5537
40.0000	-.2996
50.0000	.8445
60.0000	1.6774
70.0000	2.0778
80.0000	2.0550
90.0000	1.6637
100.0000	.9113
110.0000	-.0036
120.0000	-1.1131
130.0000	-2.2991
140.0000	-3.4442
150.0000	-4.5517
160.0000	-5.4557
170.0000	-6.2006
180.0000	-6.7716

Example :

α	$u_\alpha(\theta)$
0.0300	-15.727441289893254
0.0200	-15.728605175805426 4
0.0010	-15.729744356087332 0
0.0001	-15.730029291203653 6
0.0001	-15.730049263829984 4
0.4000	-15.730

Table 7: u_F is the Green's function of the radial displacement tabuled by Farrell (1972), u_α, the value of the same Green's function computed with a disk factor of radius α.

$\theta = 180$ degree $u_F(\theta) = -6.663$

α, deg	$u_\alpha(\theta)$
8	-6.604
7	-6.630
6	-6.653
5,5	-6.663
4	-6.688

$\theta = 170$ degree $u_F(\theta) = -6.161$

α, deg	$u_\alpha(\theta)$
8	-6.101
7	-6.122
6	-6.143
5	-6.161
4	-6.175

$\theta = 100$ degree $u_F(\theta) = 0.920$

α, deg	$u_\alpha(\theta)$
5	0.938
4	0.930
3	0.923
2,5	0.920
2	0.917

Table 8: Comparison between the Green's functions of the radial displacement obtained by the raw sum (u_R), tabuled by Farrell (u_F) and using the Boussinesq's approximation (u_B).

θ, deg.	$u_R(\theta)$	$u_F(\theta)$	$u_B(\theta)$
0.0001	-33.99	-33.64	-34.00
0.001	-33.86	-33.56	-34.00
0.01	-32.65	-31.75	-34.00
0.02	-31.80	-30.86	-34.00

2.2.4. Alternative method for small angular distances

For angular distances smaller than 0°02, the methods for series convergence acceleration developed by Farrell (1972) and presented above, cannot be applied. Indeed, in this case, the interval of alternation is so big that the 10 000 first Legendre polynomials have all the same sign. Farrell (1972) suggests to compute the Green's function for small angles replacing the sum by an integral. To numerically evaluate this integral, he suggested the Simpson's rule. Other methods have also been used. We have obtained almost the same results as using the raw summation (see Table 8). In this table, our computations are also compared with Farrell's published results. There are big differences between both sets of values. Nevertheless, Farrell's results could be reproduced by extrapolation. In order to select between all these results, the Boussinesq's solution for a plane approximation, appropriate in the small angles case, can be used. One can see in Table 8 that these results are much closer to our results without extrapolation than to Farrell's ones. It must be mentioned that the Boussinesq's solution appears to be constant because of the normalisation introduced as Farrell did.

A second argument in favour of our results is the study of errors propagation. The absolute error on the final result is deduced from the precision of the Love numbers because the other are negligeable.

For example, the absolute error on the Green's function u_r given by equation (8) is computed using the rules of sums and products of errors. An error on one Love number, $e_{h'n}$ and an error of one Legendre polynomial e_{Pn} are propagated as follows:

$$e_{ur} = \frac{a}{m_e} \sum_{n=0}^{10000} (e_{h'n} + 2e_{h'\infty}) P_n(\cos\theta)$$

$$+ \frac{a}{m_e} \sum_{n=0}^{\infty} (h'_n - h'_\infty)\, e_{P_n}$$

considering that the errors on P_n are practically zero and using $5\ 10^{-4}$ for $e_{h'n}$ and $e_{h'\infty}$ (see above, section 2.1), e_{ur} is evaluated at $1.5\ 10^{-17}$ m for unnormalised values. For examples, for $\theta = 0.0001°$ and $\theta = 0.02°$, this gives maximum relative errors of $5\ 10^{-6}$ and 10^{-3}, respectively. Up to an angle of 0.02°, the raw summation gives then sufficiently precise results. From the angle 0.1° there are sufficient alternations to use the Euler's transformation. The problem arises for the angular distances comprised between 0.02° and 0.1°. This is because, firstly, the relative error can be bigger than 10^{-3} so that the raw summation would not be appropriate; secondly, for these angles, the number of alternations is not sufficient to use the Euler's transformation, for the required precision. One can thus not select between both solutions. We decide to take the same solution as Farrell i.e. Euler's transformation until the precision on the load Love numbers increases.

2.3. Conclusion and strategy

Theoretically, the methods developed by Farrell are very advisable, but, on the basis of numerical tests, some criticisms can be formulated.

First, we reject the disk factor artifice because it has been introduced to speed up the convergence and decrease the number of operations in the computer. This reduced the computer time and this is no more necessary at present. Moreover, as previously shown, this procedure is not quite correct mathematically.

Secondly, the Euler's transformation causes some troubles for the small angular distances as well as for the large ones. The small angular distances are divided into different categories. For angles less than 0.02°, we recommand to use the Kummer's transformation alone because the alternation intervals are too large to apply the Euler's transformation. Moreover, the integral method proposed by Farrell does not improve anything. Farrell's results have probably been obtained by extrapolation and are unreliable compared to the results of the Boussinesq's plane approximation. Between 0.02° and 0.1°, the situation is much more embarrassing because the raw summation is not precise enough while there are no sufficient alternations for the Euler's transformation. As Farrell, we use the Euler's transformation. For angular distances larger than 0.1°, there is no problem for the Euler's transformation up to 100°. For angles over 100°, differences at the second or third decimal could be noted when using different choices of alternation interval (Farrell's formula or sign test). This had no influence for smaller angular distances because the choice of alternance intervals does not change much the partial sums as they contain a large number of terms. In our tables, the Farrell's intervals are used. This choice is led by the fact that for a given precision the results are obtained by using much less partial sums with respect to the number of intervals constructed on the sign test, although this is not the most logical choice. The whole strategy adopted is presented in Table 9.

In order to solve the problem for the small angular distances (between 0.02° and 0.1°), much more and more precise Love numbers must be provided. It should then be possible to apply the raw summation to angles larger than 0.02°. It must be mentioned at this point that, in practice, the Green's functions corresponding to angular distances smaller than 0.1° are generally not used except for the stations close to the coast (distance $\leq$ 10km). For these stations, the Farrell's method is no more reliable because the cells are too large in the corange and cotidal maps.

To solve the problem of the large angular distances, we should concentrate our efforts to find another method to sum alternate series.

3. NUMERICAL RESULTS

Computer programs setting up the strategy discussed above have been developed at the Royal Observatory of Belgium (Francis, 1987). They allow us to compute the Green's functions using the same rheological property profiles inside the Earth as Farrell i.e. the Guttenberg-Bullen profile (G-B). The results presented in Table 10 are compared with Farrell's ones.

Other rheological profiles e.g. the 1066A model (Gilbert & Dziewonski, 1975) or the PREM (Dziewonski, 1981), have been integrated by respectively Xianhua (1986) and Zschau and Rabbel (personal communication to Melchior, 1982) in order to obtain load Love numbers. New Green's functions are computerized using these different inputs. The results are presented in Table 11 and plotted in Figure 4.

TABLE 9: Strategy for the computation of the Green's function

1) Kummer's transformation is applied;

2) no disk factor is used;

3) Euler's transformation or raw summation?

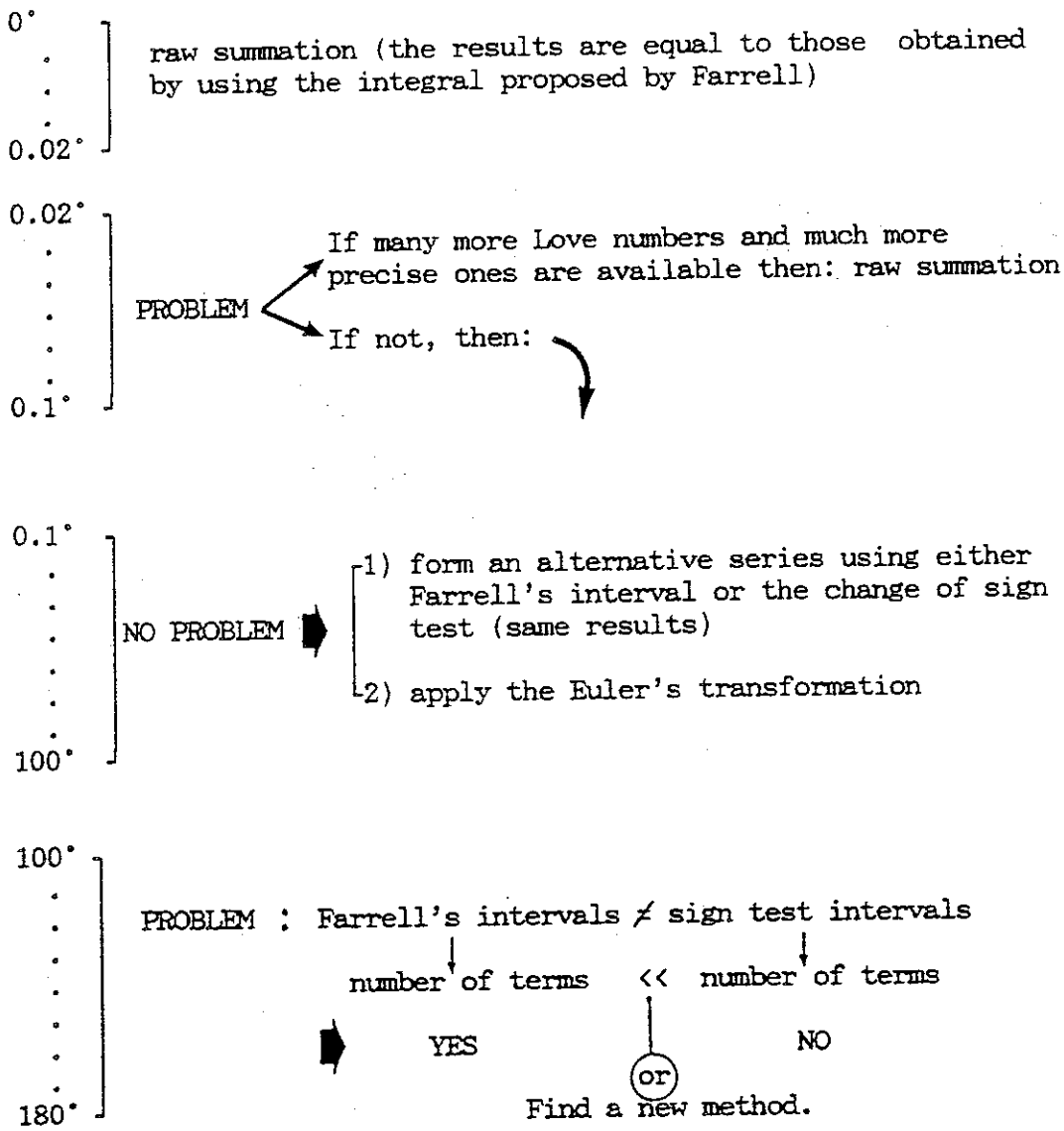

Table 10: Green's functions for the Gutenberg-Bullen profile (Francis, 1987).

θ (°)	$u(\theta)$	$v(\theta)$	$g^E(\theta)$	$t^E(\theta)$	$A^E(\theta)$
.0001	-33.991	-11.367	-78.802	34.006	.000
.0010	-33.857	-11.366	-78.481	34.005	.000
.0100	-32.651	-11.289	-75.632	33.764	.005
.0200	-31.801	-11.177	-73.782	33.981	.010
.0300	-30.983	-11.125	-72.013	33.727	.015
.0400	-30.120	-11.056	-70.111	33.688	.019
.0600	-28.475	-10.944	-66.484	33.343	.029
.0800	-26.886	-10.634	-62.931	32.997	.037
.1000	-25.424	-10.367	-59.669	32.396	.045
.1600	-21.818	-9.372	-51.486	29.844	.067
.2000	-20.037	-8.726	-47.351	27.786	.078
.2500	-18.381	-8.026	-43.403	25.283	.091
.3000	-17.199	-7.470	-40.483	23.117	.102
.4000	-15.730	-6.731	-36.640	19.867	.122
.5000	-14.931	-6.343	-34.352	17.873	.143
.6000	-14.430	-6.164	-32.814	16.875	.165
.8000	-13.689	-6.061	-30.573	16.347	.214
1.0000	-12.999	-5.989	-28.706	16.270	.265
1.2000	-12.316	-5.860	-27.026	16.207	.314
1.6000	-10.972	-5.478	-23.983	15.928	.403
2.0000	-9.761	-4.999	-21.373	15.033	.476
2.5000	-8.520	-4.391	-18.733	13.640	.546
3.0000	-7.543	-3.865	-16.650	12.368	.600
4.0000	-6.136	-3.069	-13.606	10.116	.677
5.0000	-5.248	-2.523	-11.598	8.255	.728
6.0000	-4.671	-2.158	-10.211	6.948	.770
7.0000	-4.280	-1.916	-9.205	5.974	.811
8.0000	-4.003	-1.759	-8.446	5.279	.855
9.0000	-3.799	-1.653	-7.853	4.755	.903
10.0000	-3.641	-1.580	-7.375	4.374	.957
12.0000	-3.399	-1.501	-6.638	3.915	1.080
16.0000	-3.004	-1.438	-5.571	3.556	1.368
20.0000	-2.624	-1.388	-4.740	3.365	1.679
25.0000	-2.112	-1.311	-3.821	3.333	2.077
30.0000	-1.537	-1.212	-2.962	3.320	2.449
40.0000	-.296	-.929	-1.437	2.966	2.916
50.0000	.845	-.590	-.290	1.949	2.782
60.0000	1.674	-.321	.369	.421	2.004
70.0000	2.078	-.218	.537	-1.263	.732
80.0000	2.050	-.305	.318	-2.706	-.783
90.0000	1.637	-.554	-.143	-3.713	-2.290
100.0000	.913	-.897	-.729	-4.262	-3.584
110.0000	-.036	-1.252	-1.369	-4.416	-4.539
120.0000	-1.131	-1.547	-2.012	-4.221	-5.097
130.0000	-2.291	-1.718	-2.615	-3.736	-5.248
140.0000	-3.442	-1.726	-3.144	-3.065	-4.998
150.0000	-4.517	-1.548	-3.592	-2.517	-4.356
160.0000	-5.457	-1.186	-3.966	-1.567	-3.322
170.0000	-6.206	-.658	-4.282	-.816	-1.879
180.0000	-6.716	.000	-4.555	.000	.000

Table 11: Gravimetric Green's function for the Gutenberg-Bullen, 1066A and PREM models, respectively.

θ, deg.	g_{G-B}	g_{1066A}	g_{PREM}
.0001	-78.802	-188.497	-98.084
.0010	-78.481	-187.381	-97.663
.0100	-75.632	-176.498	-93.464
.0200	-73.782	-166.009	-88.856
.0300	-72.013	-155.053	-84.351
.0400	-70.111	-144.647	-79.986
.0600	-66.484	-124.910	-71.818
.0800	-62.931	-106.973	-64.562
.1000	-59.669	-91.767	-58.335
.1600	-51.486	-61.289	-45.568
.2000	-47.351	-50.423	-40.854
.2500	-43.403	-43.063	-37.487
.3000	-40.483	-39.566	-35.637
.4000	-36.640	-36.822	-33.721
.5000	-34.352	-35.464	-32.508
.6000	-32.814	-34.363	-31.434
.8000	-30.573	-32.259	-29.495
1.0000	-28.706	-30.080	-27.728
1.2000	-27.026	-28.177	-26.167
1.6000	-23.983	-24.842	-23.569
2.0000	-21.373	-21.992	-21.311
2.5000	-18.734	-19.116	-18.555
3.0000	-16.650	-16.878	-16.476
4.0000	-13.606	-13.641	-13.528
5.0000	-11.598	-11.543	-11.451
6.0000	-10.211	-10.128	-9.859
7.0000	-9.205	-9.144	-8.889
8.0000	-8.446	-8.423	-8.023
9.0000	-7.853	-7.873	-7.466
10.0000	-7.375	-7.437	-6.949
12.0000	-6.637	-6.761	-6.212
16.0000	-5.571	-5.705	-5.138
20.0000	-4.739	-4.812	-4.298
25.0000	-3.821	-3.849	-3.391
30.0000	-2.962	-2.977	-2.566
40.0000	-1.437	-1.382	-1.126
50.0000	-.290	-.199	-.078
60.0000	.369	.456	.483
70.0000	.536	.605	.577
80.0000	.318	.376	.331
90.0000	-.143	-.107	-.146
100.0000	-.728	-.717	-.733
110.0000	-1.369	-1.359	-1.345
120.0000	-2.012	-1.970	-1.928
130.0000	-2.615	-2.524	-2.455
140.0000	-3.145	-3.007	-2.916
150.0000	-3.593	-3.423	-3.314
160.0000	-3.966	-3.781	-3.656
170.0000	-4.282	-4.089	-3.954
180.0000	-4.555	-4.354	-4.209

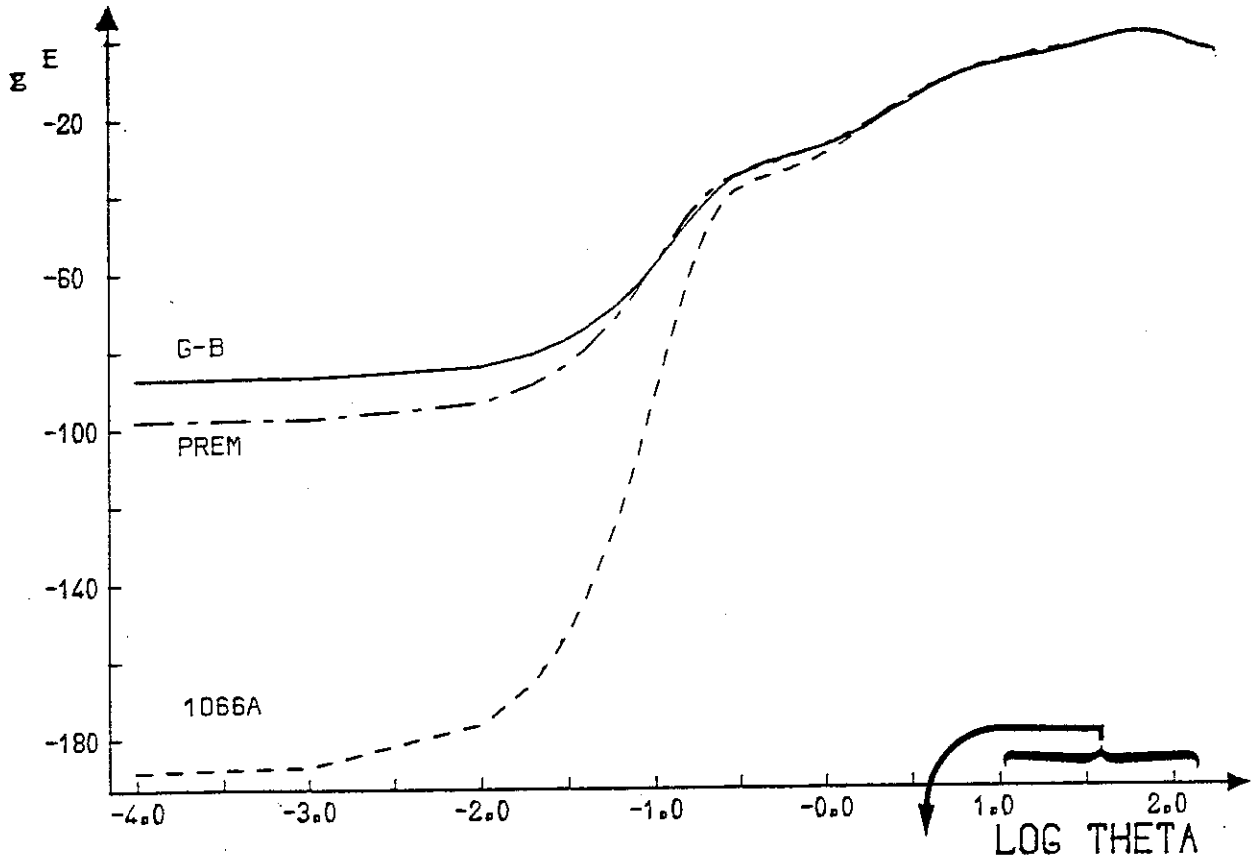

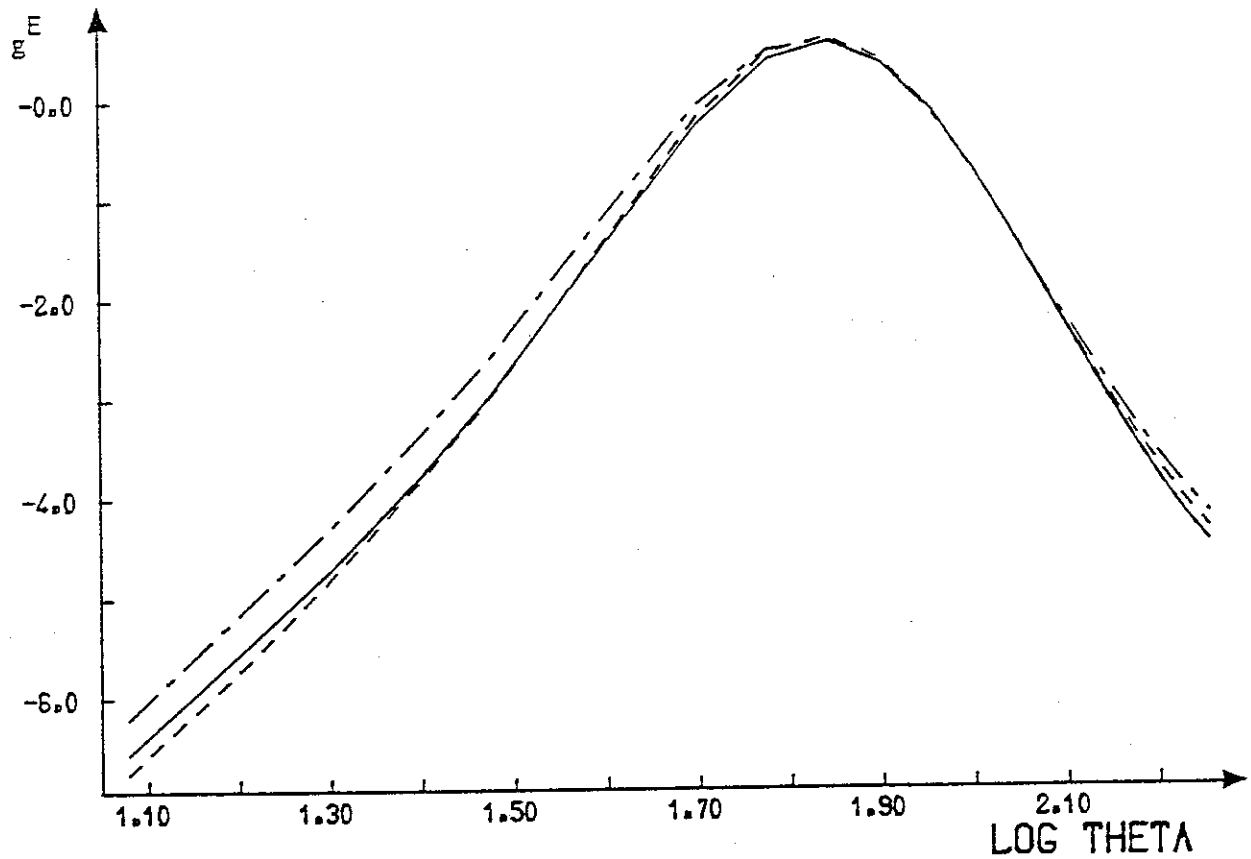

Figure 4: Gravity Green's functions for different models.

Convolutions between these resulting Green's functions and the complex vector representing the ocean tide amplitudes and phases are performed at five stations as examples. From the comparison between the results of the three different models (Table 12) it can be concluded for gravity that:

1) There are practically no differences between the G-B model and the 1066A, although the Green's functions are very different for small angular distances (Figure 4). This small influence is normal because, as already mentioned, the small angular distance Green's functions are only used for coastal stations.

2) However, the differences are more important for the PREM model. This is due to the systematic difference between G-B - and PREM- Green's functions.

The new theoretical results for the ocean indirect effects are very promising because the new residuals are much smaller. In the future, we plan to recompute all the residuals for all the stations available at the ICET, using the Green's functions of the new PREM model or of the Zschau's new inelastic model (Zschau and Wang, 1985).

Acknowledgements

We are thankful to B. Ducarme for reading our manuscript and for all the scientific discussions we had. Prof. P. Melchior is greatfully acknowledged for bringing us into this field and reading our manuscript.

All the computations have been performed at the Royal Observatory of Belgium.

Table 12 : Tidal wave M_2. Gravity load vectors $\vec{L}$ have been computed from the Schwiderski maps according Farrell's procedure for three models : Gutenberg-Bullen, 1066A and PREM. The results are compared to the observed residues. The amplitudes of $\vec{L}$ are given in microgals in the first column and the phases of $\vec{L}$ in degrees in the second.

Station	Lat.	Lon.	$\vec{L}$(G-B)		$\vec{L}$(1066A)		$\vec{L}$(PREM)		Observed residues	
Brugge	51.20	3.22	1.9036	76.67	1.9036	77.41	1.8287	75.63	2.69	72.
Bruxelles	50.80	4.36	1.8797	63.07	1.8884	63.50	1.8069	62.80	1.76	61.4
Walferdange	49.66	6.15	1.8381	60.80	1.8550	60.99	1.7640	60.61	1.63	52.
Potsdam	52.38	13.07	1.1426	45.69	1.1596	45.73	1.0873	45.45	0.99	44.6
Kiev	50.40	30.60	0.6314	11.84	0.6350	11.56	0.5902	11.65	1.06	12.5

References

Dehant, V. & Ducarme, B., 1987: "Comparison between the theoretical and observed tidal gravimetric factors".
Phys. Earth Planet.Int.,accepted for publication.

Dziewonski A.M. & Anderson D.L., 1981: "Preliminary reference Earth Model".
Phys. Earth Planet.Int., 25, 297-356

Farrell W.E., 1972: "Deformation of the Earth by Surface Loads".
Reviews of geophysics and Space Physics, vol.10, N°3, 761-797.

Francis, O., 1987: "Calcul numérique de la déformation de la croûte terrestre sous l'effet d'une charge en surface".
Mémoire de l'Université Catholique de Louvain, Belgium, 79 pp.

Gilbert, F. & Dziewonski, A.M., 1975: "An application of normal mode theory to the retrieval of structural parameters and source mechanisms from seismic spectra".
Phil.Trans. R. Soc. London A, 278, pp 187-269

Melchior, P., 1983: "The Tides of the Planet Earth".
2nd ed., Pergamon Press, Oxford, 641 pp.

Xianhua, J., 1986: "Static deformation Response of the Earth to tidal potential, concentrated mass loading and shear stress".
B.I.M., 97, pp 6587-6597.

Zschau, J. & Wang, R., 1985: "Imperfect elasticity in the Earth's mantle: implications for Earth tides and Long period deformation"
Proceedings 10th International Symposium on Earth Tides, Madrid, Spain, pp 379-384